Electronic Photodepletion Spectroscopy of Dibenzo-18-crown-6 with a Potassium Ion

Hwan Jin Kim, Won Jik Shin, Chang Min Choi, Jun Ho Lee, and Nam Joon Kim[*]

Department of Chemistry, Chungbuk National University, Chungbuk 361-763, Korea. [*]E-mail: namjkim@chungbuk.ac.kr
Received July 25, 2008

Electronic photodepletion spectrum of dibenzo-18-crown-6 with a potassium ion (K⁺-DB18C6) was obtained in the gas phase using electrospray ionization and quadrupole ion-trap reflectron time-of-flight mass spectrometry. The spectrum exhibited rather a broad absorption band at 36350 cm⁻¹, which was tentatively assigned as the origin of the S_1 band. The photodepletion spectrum of Cs⁺-DB18C6 was also obtained to elaborate the effects of metal cations on electronic and geometric structures of metal cation-DB18C6 complexes. We found that the S_1 band of Cs⁻-DB18C6 was red-shifted by 180 cm⁻¹ from that of K⁺-DB18C6. With the results of quantum theoretical calculations using the density functional theory, we suggested that the red-shift arose mainly from weaker binding of Cs⁺ to DB18C6 than that of K⁻, which resulted from a larger size of Cs⁺ than that of the cavity in DB18C6.

Key Words : Photodepletion spectrum, Electrospray ionization, Dibenzo-18-crown-6, Quadrupole ion trap

Introduction

Molecular sensors have strong affinity to specific molecules or ions and in most cases, their physical and chemical properties change significantly upon binding to them.[1] Crown ethers, first synthesized by Charles Pederson in 1967,[2,3] are one of the well-known molecular sensors for metal cations. The first crown ethers are 18-crown-6 (18C6) and dibenzo-18-crown-6 (DB18C6) (Scheme 1). They were reported to have strong affinity to the metal cations whose radii were similar to their cavity sizes. For example, 18C6 exhibited the strongest binding affinity to a potassium ion (K⁺), the radius of which was the closest to the cavity size among other alkali metal cations.[4] However, other factors were also known to contribute to the selective binding of crown ethers such as solvation enthalpies and entropies of the cations, the number of donor atoms of a crown ether participating in the binding to a metal cation, and the conformational difference between the bound and unbound crown ethers.[5]

Many derivatives of crown ethers of different binding selectivity have also been synthesized.[6] Misumi and co-workers[7] synthesized a crowned di-nitrophenyl-azophenol that changed its color by binding to Li⁺. Kim and coworkers[8] reported the synthesis of calix-azacrown-ethers which had the selectivity for K⁻ and changed their colors when they bound with K⁺. De Silva *et al.*[9] also studied crown ethers which emitted fluorescence when they bound with a specific ion. The changes in physical and chemical properties of crown ethers upon complexation with various cations have been investigated using fluorescence spectroscopy or nuclear magnetic resonance spectroscopy.[10-12]

However, most of these studies have been carried out in solution phase, where the interactions with solvents or other species in solution cannot be excluded and may affect the physical and chemical properties of crown-ether complex ions. Therefore, to elucidate the intrinsic nature of crown-ether complex ions, it is critical to investigate them in isolated gas phase.

The advent of an electrospray ionization (ESI) technique combined with mass spectrometry[13] provides a powerful tool to study the mass-selected crown-ether complex ions in the gas phase. Gas-phase selectivity of crown ethers was investigated using the kinetic method.[14] They generated ion complexes of crown ethers with two different alkali metal cations and measured relative abundance of their product ions following high-energy dissociation. Intrinsic cation affinities and complexation rates for alkali metal cations of crown ethers were measured following ion-molecule reactions in the gas phase.[15] Bond-dissociation energies of gas-phase crown ether complexes with alkali metal cations were determined from the thresholds of collision-induced dissociation obtained using guided ion beam mass spectrometry.[16] Recently, Ebata and coworkers[17] reported the laser-induced fluorescence spectra of jet-cooled benzo-18-crown-6, dibenzo-18-crown-6 and their hydrated complexes. However, spectroscopic studies on gas-phase crown ether complexes with alkali metal cations, which may reveal their photo-physical and -chemical properties, have never been performed, as far as we know.

In this paper, we obtained the first electronic photodepletion spectrum of DB18C6 complexes with K⁺ using ESI and quadrupole ion trap reflectron time-of-flight mass spectrometry (QIT-reTOF). DB18C6 was chosen because it has benzene rings as a chromophore for ultraviolet light
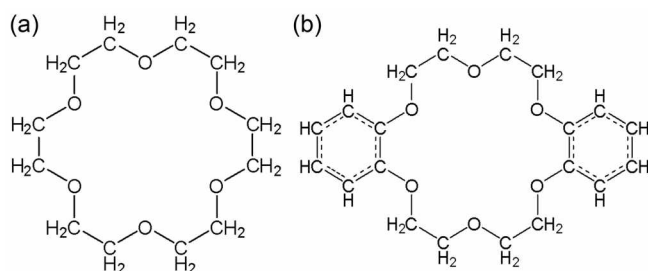
Scheme 1

(UV). Moreover, with the proximity of the benzene rings to the cavity of DB18C6, the interactions between DB18C6 and metal cations can be closely monitored by UV absorption spectroscopy of the complex ions.

To know how the metal cations of different characters affect geometric and electronic structures of the complex ions, the photodepletion spectrum of Cs^+-DB18C6 was also obtained and compared with that of K^--DB18C6. The red-shift of the first singlet excitation band (S_1) of Cs^+-DB18C6 from that of K^+-DB18C6 was observed and explained with the results of theoretical calculations performed using the density functional theory (DFT).

Experimental Methods

The details of our experimental set-up were reported previously[18] and only a brief description will be given.

The powder samples of DB18C6, KCl, and CsCl were purchased from Aldrich and used without further purification. Each powder sample was dissolved in methanol at a concentration of 200 μM. The solution of DB18C6 was then mixed with the same volume of the KCl and CsCl solution to produce K^+- and Cs^+-DB18C6, respectively. Each of the mixed solutions was electro-sprayed into ion droplets through a nozzle floated to +3 kV. The ion droplets evaporated their solvent molecules while passing through a heated capillary. The desolvated ions entered into the main chamber through a skimmer and then trapped in a QIT. A liquid nitrogen reservoir was placed on top of the QIT to lower the temperature down to 150 K.

After 90 ms of ion storage, UV laser pulses (~2 mJ/pulse) were irradiated onto the ions in the QIT for photodissociation. Then, a positive (+1290 V) and a negative DC pulse (−340 V) were applied to the entrance and exit endcap of the QIT, respectively, to extract all fragment and parent ions out to the field-free region of reflectron TOFMS for mass analysis. The ions passing through the field-free region were reflected in the reflectron and detected by micro-channel plate. The ion signals were processed and stored by a digital storage oscilloscope. The timings of the trapping, the laser firing, and the application of the extraction DC pulses were all synchronized using a digital delay generator.

Fluorescein 548 was used as a dye to generate visible light in the wavelength range of 544-576 nm from a dye laser pumped by the second harmonic of an Nd:YAG laser. The visible light was converted into UV beams by second harmonic generation with a BBO crystal.

Theoretical Methods

The structures of K^-- and Cs^+-DB18C6 in the electronic ground state were optimized using DFT at the B3LYP/6-31+G(d) level. LANL2DZ was used as a basis set for K and Cs. The singlet excitation energies at the optimized structures were predicted using TD-DFT at the same level of theory. All calculations were performed using the GAUSSIAN 03 package.[19]
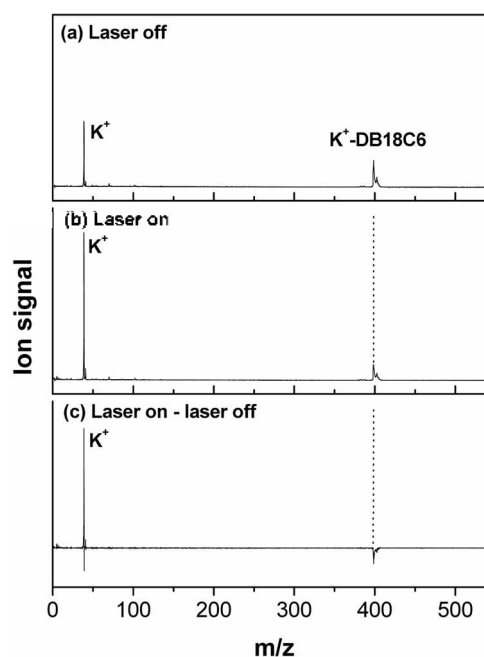

Figure 1. Mass spectra of K^--DB18C6 (a) without and (b) with irradiation of laser pulses at 275 nm. (c) Difference mass spectrum obtained by subtracting the laser-off signals from the laser-on.

Results and Discussion

Figure 1a shows the mass spectrum of K^+-DB18C6 obtained in the QIT-reTOF. Only the ion signals of K^+ and K^+-DB18C6 were observed in the spectrum. One possible source of K^- is meta-stable dissociation of K^+-DB18C6 and the other is unbound K^+ ions in the K^+-DB18C6 solution. Figure 1b is the mass spectrum obtained with irradiation of laser pulses at 275 nm onto the ions trapped in the QIT. Figure 1c shows the difference spectrum obtained by subtracting the laser-off signals (Fig. 1a) from the laser-on (Fig. 1b). The negative signal, therefore, represents the intensity of depleted ions and the positive one shows the fragment-ion intensity generated by photo-induced dissociation (PID).

The difference spectrum indicates that K^--DB18C6 dissociates to produce K^+ following absorption of laser pulses at 275 nm. This was also true at other wavelengths where K^+-DB18C6 has the absorption. The larger ion signal of the fragment K^+ than that of the depleted K^--DB18C6 was attributed to mass-dependent ion trapping and detection efficiency of QIT-reTOF.

Figure 2a shows the electronic photodepletion spectrum of K^--DB18C6 in the wavenumber region of 34900-36810 cm^{-1}. The spectrum was calibrated against the variation of laser fluence over the frequency. It is likely that the excitation-energy dependence of the photodepletion yield results mainly from the energy dependence of molecular absorption probability.[20] Therefore, we assumed that the photodepletion spectra exhibited the same spectral feature as the electronic absorption spectra.[21,22] The photodepletion spectrum of K^--DB18C6 showed rather a broad absorption band at 36350 cm^{-1}. Since no other bands appeared at longer
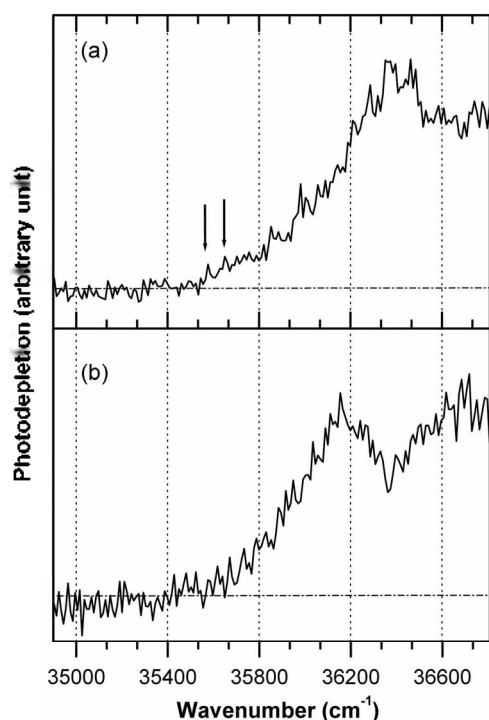
Figure 2. Electronic photodepletion spectra of DB18C6 complex ions with (a) K⁻ and (b) Cs⁻. The arrows indicate the 0-0 bands of two different conformers of bare DB18C6 (ref. 17). The base lines were represented with a dash-dot line.

wavelength region, we tentatively assigned it as the origin of the first singlet excitation band (S_1).

The spectrum of Cs⁻-DB18C6 (Fig. 2b) was also obtained to know how the nature of the metal cation bound to DB18C6 affects the spectral feature of the complex ions. Different from the spectrum of K⁻-DB18C6, that of Cs⁺-DB18C6 exhibited two absorption bands in the same wavelength region. The lowest-energy band was at 36170 cm⁻¹ and the two bands were ~500 cm⁻¹ apart. As the previous assignment,[11] we assigned the second band as a vibronic band revealing the vibrational structure of the S_1 state. It is noteworthy that the first absorption band of Cs⁺-DB18C6 is red-shifted by 180 cm⁻¹ from that of K⁻-DB18C6. The red-shift has not drawn much attention because it is not clearly observable in the solution-phase spectra.

In order to know the cause of the red-shift, quantum theoretical calculations were carried out using DFT at the B3LYP/6-31+G(d) level. Figure 3 shows the optimized structures of K⁻- and Cs⁺-DB18C6 in the electronic ground state, which agree well with previous reports.[23,24] The lowest excitation energy of K⁻- or Cs⁺-DB18C6 at the optimized geometry was predicted by TD-DFT at the same level of theory and plotted in Figure 4. It is remarkable that the red-shift of the S_1 band of Cs⁻-DB18C6 from that of K⁺-DB18C6 is also predicted in the theoretical calculations.

Those experimental and theoretical results show that the metal cations bound in the cavity of DB18C6 play critical roles in determining stable geometries of the complex ions and thereby affect their electronic structures as well. The
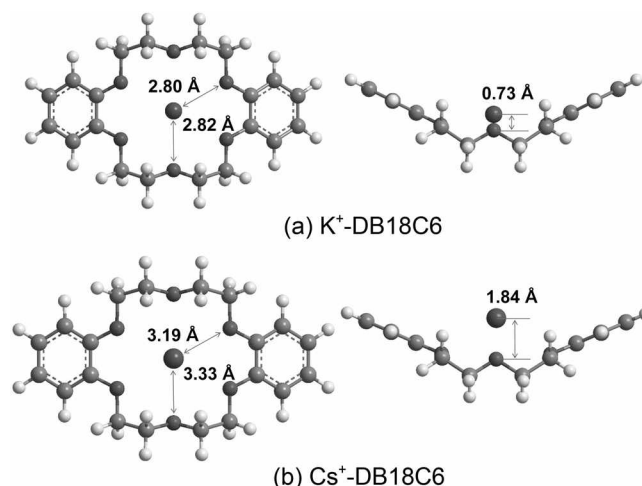

Figure 3. Optimized structures of DB18C6 complexes with (a) K⁻ and (b) Cs⁻ in the electronic ground state obtained using DFT at the B3LYP/6-31+G(d) level.
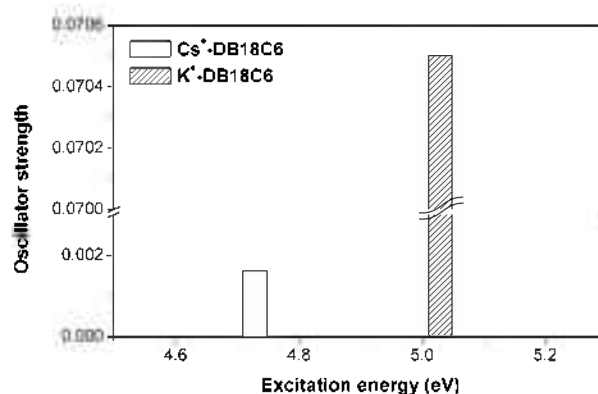
Figure 4. Plot of the singlet excitation energies (S_1) of K⁻- and Cs⁻-DB18C6 calculated using TD-DFT at the B3LYP/6-31+G(d) level.

variation of the energies of the first absorption bands indicates the change in relative energies of HOMO (highest occupied molecular orbital) and LUMO (lowest unoccupied molecular orbital). Since the S_1 bands of K⁻- and Cs⁻-DB18C6 arise from the $\pi\pi^*$ transition involving electrons in the π and π^* orbitals of the benzene rings in DB18C6, the relative energies of the π and π^* orbitals determine the energies of the S_1 bands.

Therefore, we can explain the reason for the red-shift as follows. The cavity radius of DB18C6 is not known, but the radius of 18C6, which is about the same as that of DB18C6, is 1.34-1.43 Å.[25] This is very close to the ionic radius of K⁻ (1.38 Å), but much smaller than that of Cs⁺ (1.67 Å).[26,27] Accordingly, in the optimized geometries, Cs⁺ is located at 1.84 Å above the cavity plane made of the six oxygen atoms, while K⁻ sits almost inside the cavity (Fig. 3). In those structures, the distances from the six oxygen atoms to Cs⁻ are much longer than those to K⁺. Since the metal cations are practically bound to the six oxygen atoms acting as electron donors in the complex ions, the lengthening of the distance will cause weaker binding of Cs⁻ to DB18C6 than that of K⁺.[24] Therefore, the stabilization of the π orbital is expected
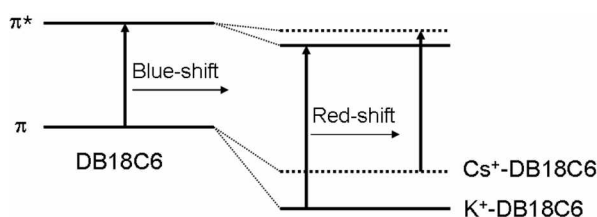
Figure 5. Schematic energy diagram illustrating the red-shift of the S_1 band of Cs^--DB18C6 from that of K^--DB18C6.

to be less upon forming the DB18C6 complex ions with Cs^+ than that with K^-.

Since the excitation energy to the S_1 band is determined by the relative energy of both π and π^* orbital, we need to know how the energy of the π^* orbital as well as that of the π orbital changes upon complexation with the metal cations. However, considering that the S_1 bands of both K^-- and Cs^+-DB18C6 are blue-shifted from the 0-0 band of bare DB18C6 (Fig. 2),[17] we may insist that the stabilization of the π^* orbital upon forming the complex ions is less than that of the π orbital. This is further supported by the pictorial representations of the π and π^* orbitals (not shown here), which show that the orbitals of the four oxygen atoms near the benzene rings become smaller in the π^* than in the π orbital. Thus, with the reduced strength of the interactions between the π^* orbitals and the metal cations, the difference in energies of the π^* orbitals between K^-- and Cs^+-DB18C6 will be smaller than that of the π orbital. Therefore, we suggest that a larger difference in energies of the π orbitals between K^+- and Cs^--DB18C6 compared to that of the π^* orbitals and also weaker binding of Cs^+ to DB18C6, leading to less stabilization of both the π and π^* orbitals than that of K^-, result in a smaller energy gap between the π and π^* orbitals of Cs^+-DB18C6 than that of K^--DB18C6 (Fig. 5).

Conclusions

Electronic photodepletion spectra of K^+- and Cs^+-DB18C6 were obtained in isolated gas phase and investigated with the help of theoretical calculations using DFT and TD-DFT. The red-shift of the S_1 band was observed upon changing the metal cation bound to DB18C6 from K^+ to Cs^-. We suggest that the relative size of metal cations with respect to the cavity size plays a critical role in determining the stable geometries of the complex ions and thereby affects their electronic structures. With a larger size of Cs^+ than that of the cavity, Cs^- sits far above the cavity. In contrast, K^- fits inside the cavity with its almost identical radius to that of the cavity. Those structures result in weaker binding of Cs^+ than that of K^- toward DB18C6, which is mainly responsible for the red-shift of the S_1 band of Cs^+-DB18C6 from that of K^+-DB18C6. The studies of DB18C6 complexes with other alkali and alkaline earth metal cations are under way to investigate the host-guest interactions in more detail using metal cation-DB18C6 complexes as a model system.

References

1. Cerrie, W.; Rogers, W. O.; Michael, W. O. *Coord. Chem. Rev.* **2002**, *233*, 341.
2. Pedersen, C. J. *J. Am. Chem. Soc.* **1967**, *89*, 7017.
3. Pedersen, C. J. *Science* **1988**, *241*, 536.
4. Gokel, G. W.; Leevy, W. M.; Weber, M. E. *Chem. Rev.* **2004**, *104*, 2723.
5. Gokel, G. W.; Goli, D. M.; Minganti, C.; Echegoyen, L. *J. Am. Chem. Soc.* **1983**, *105*, 6786.
6. Kim, J.-K.; Seo, J. J.; Yim, E. S.; Jin, Y.; Song, S.; Suh, H. *Bull. Kor. Chem. Soc.* **2008**, *29*, 1069.
7. Nakashima, K.; Nakatsuji, S.; Akiyama, S.; Kaneda, T.; Misumi, S. *Chem. Lett.* **1982**, *11*, 1781.
8. Kim, J. S.; Shon, O. J.; Ko, J. W.; Cho, M. H.; Yu, I. Y.; Vicens, J. *J. Org. Chem.* **2000**, *65*, 2386.
9. De Silva, A. P.; Gunaratne, H. Q. N.; Gunnlaugsson, T.; Huxley, A. J. M.; McCoy, C. P.; Rademacher, J. T.; Rice, T. E. *Chem. Rev.* **1997**, *97*, 1515.
10. Christensen, J. J.; Eatough, D. J.; Izatt, R. M. *Chem. Rev.* **1974**, *74*, 351.
11. Shizuka, H.; Takada, K.; Morita, T. *J. Phys. Chem.* **1980**, *84*, 994.
12. Wilson, M. J.; Pethrick, R. A.; Pugh, D.; Islam, M. S. *J. Chem. Soc. Faraday Trans.* **1997**, *93*, 2097.
13. Yamashita, M.; Fenn, J. B. *J. Phys. Chem.* **1984**, *88*, 4451.
14. Maleknia, S.; Brodbelt, J. *J. Am. Chem. Soc.* **1992**, *114*, 4295.
15. Chu, I.-H.; Zhang, H.; Dearden, D. V. *J. Am. Chem. Soc.* **1993**, *115*, 5736.
16. More, M. B.; Ray, D.; Armentrout, P. B. *J. Am. Chem. Soc.* **1999**, *121*, 417.
17. Kusaka, R.; Inokuchi, Y.; Ebata, T. *Phys. Chem. Chem. Phys.* **2007**, *9*, 4452.
18. Yoon, T. O.; Choi, C. M.; Kim, H. J.; Kim, N. J. *Bull. Korean Chem. Soc.* **2007**, *28*, 619.
19. Frisch, M. J.; Trucks, G. W.; Schlegel, H. B.; Scuseria, G. E.; Robb, M. A.; Cheeseman, J. R.; Montgomery, J. A. Jr.; Vreven, T.; Kudin, K. N.; Burant, J. C.; Millam, J. M.; Iyengar, S. S.; Tomasi, J.; Barone, V.; Mennucci, B.; Cossi, M.; Scalmani, G.; Rega, N.; Petersson, G. A.; Nakatsuji, H.; Hada, M.; Ehara, M.; Toyota, K.; Fukuda, R.; Hasegawa, J.; Ishida, M.; Nakajima, T.; Honda, Y.; Kitao, O.; Nakai, H.; Klene, M.; Li, X.; Knox, J. E.; Hratchian, H. P.; Cross, J. B.; Adamo, C.; Jaramillo, J.; Gomperts, R.; Stratmann, R. E.; Yazyev, O.; Austin, A. J.; Cammi, R.; Pomelli, C.; Ochterski, J. W.; Ayala, P. Y.; Morokuma, K.; Voth, G. A.; Salvador, P.; Dannenberg, J. J.; Zakrzewski, V. G.; Dapprich, S.; Daniels, A. D.; Strain, M. C.; Farkas, O.; Malick, D. K.; Rabuck, A. D.; Raghavachari, K.; Foresman, J. B.; Ortiz, J. V.; Cui, Q.; Baboul, A. G.; Clifford, S.; Cioslowski, J.; Stefanov, B. B.; Liu, G.; Liashenko, A.; Piskorz, P.; Komaromi, I.; Martin, R. L.; Fox, D. J.; Keith, T.; Al-Laham, M. A.; Peng, C. Y.; Nanayakkara, A.; Challacombe, M.; Gill, P. M. W.; Johnson, B.; Chen, W.; Wong, M. W.; Gonzalez, C.; Pople, J. A. *Gaussian 03*, Revision C.02; Gaussian, Inc.: Wallingford, CT, 2004.
20. Boyarkin, O. V.; Mercier, S. R.; Kamariotis, A.; Rizzo, T. R. *J. Am. Chem. Soc.* **2006**, *128*, 2816.
21. Ohashi, K.; Nishi, N. *J. Phys. Chem.* **1992**, *96*, 2931.
22. Takasu, R.; Nishikawa, K.; Miura, N.; Sabu, A.; Hashimoto, K.; Schulz, C. P.; Hertel, I. V.; Fuke, K. *J. Phys. Chem. A* **2001**, *105*, 6602.
23. Grootenhuis, P. D. J.; Kollman, P. A. *J. Am. Chem. Soc.* **1989**, *111*, 2152.
24. Anderson, J. D.; Paulsen, E. S.; Dearden, D. V. *Int. J. Mass Spectrom.* **2003**, *227*, 63.
25. Dalley, N. K.; Izatt, R. M.; Christensen, J. J. *Synthetic Multidentate Macrocyclic Compounds*; Academic: New York, 1978.
26. Shannon, R. D. *Acta Crystallogr.* **1976**, *A32*, 751.
27. Jia, Y. Q. *J. Solid State Chem.* **1991**, *95*, 184.